BULLETIN OF THE POLISH ACADEMY OF SCIENCES
TECHNICAL SCIENCES, Vol. 61, No. 4, 2013
DOI: 10.2478/bpasts-2013-0109

Quasi-analytic multidimensional signals

S.L. HAHN and K.M. SNOPEK*

Institute of Radioelectronics, Warsaw University of Technology, 15/19 Nowowiejska St., 00-665 Warsaw, Poland

Abstract. In a recent paper, the authors have presented the unified theory of n-dimensional (n-D) complex and hypercomplex analytic signals with single-orthant spectra. This paper describes a specific form of these signals called quasi-analytic. A quasi-analytic signal is a product of a n-D low-pass (base-band) real (in general non-separable) signal and a n-D complex or hypercomplex carrier. By a suitable choice of the carrier frequency, the spectrum of a low-pass signal is shifted into a single orthant of the Fourier frequency space with a negligible leakage into other orthants. A measure of this leakage is defined. Properties of quasi-analytic signals are studied. Problems of polar representation of quasi-analytic signals and of its lower rank representation are discussed.

Key words: analytic complex and hypercomplex signals, polar representation, modulation techniques, lower rank signals.

1. Introduction

Within the last twenty years, the theory of multidimensional complex and hypercomplex analytic signals has been still developing and have found various applications. For example in image analysis, the 2-D quaternion analytic signal has been used for envelope detection and feature extraction [1–3]. In [4–8], it has been shown that basing on an analytic (complex or hypercomplex) representation of a grey-scale image, it is possible to define its local amplitudes and phase functions. Moreover in [7], the problem of reconstruction of a grey-scale image from its polar representation has been studied. The newest interesting application of 2-D complex analytic signals with single-quadrant spectra is processing of SAFT (Synthetic Aperture Focusing Technique)–reconstructed images in nondestructive ultrasonic testing [9]. The hypercomplex approach has proliferated also into color image processing, for example in the domain of edge-detection filtering [10] or motion estimation [11]. We see that practical applications appear mainly in the domain of 2-D signals with spectra defined using complex or hypercomplex Fourier transforms [12–13].

The idea of comparing the 2-D complex analytic signals with quaternion analytic signals has appeared in [14], where the authors have stated that both are completely equivalent and the choice of a method is a matter of convention. Recently in [1], the theory of complex and hypercomplex analytic signals with single-orthant spectra has been unified and the problem of its extension for 3-D signals has been discussed. In this paper, we go further in our research and define and study properties of quasi-analytic energy signals, i.e., signals with spectra limited to a single orthant of the frequency space with a negligible leakage into other orthants. Let us remind that an orthant is a strictly determined part of the n-dimensional (n-D) Cartesian frequency space, e.g. in 1-D, it is a half-axe, in 2-D – a single quadrant, in 3-D – a single octant etc.

Let us recall the general frequency-domain definition of an *analytic signal* with the single–orthant (1^{st} orthant) spectrum [6–8]. Consider a real n-dimensional signal $g(\boldsymbol{x})$, $x = (x_1, x_2, \ldots, x_n) \in R^n$ and its n-dimensional complex or hypercomplex Fourier transform $G(f)$, $f = (f_1, f_2, \ldots, f_n) \in R^n$. The multiplication of the spectrum $G(\boldsymbol{f})$ by the n-D unit-step $1(\boldsymbol{f})$ yields a single-orthant spectrum in the 1^{st} orthant of the frequency space R^n. So, the n-D complex/hypercomplex *analytic signal* $\psi^{(1)}(x)$ is defined by the inverse complex / hypercomplex Fourier transform of the 1^{st} orthant spectrum (the superscript 1 denotes the orthant's label):

$$\psi^{(1)}(\boldsymbol{x}) = F^{-1}\{\mathbf{1}(\boldsymbol{f})G(\boldsymbol{f})\}. \tag{1}$$

Let us note that the spectrum support of (1) is limited to the 1^{st} orthant of the n-D frequency space. (Note: The term "support" is commonly used by mathematicians to denote the domain in which a given function is non zero. In this paper, this notion is used in the same sense.)

The $n-D$ *quasi-analytic signal* $\psi_1(x)$ is defined in the signal domain (x-domain) as

$$\psi_1(x) = g(x)\ \boldsymbol{e}^{e_1 2\pi\, f_{10}x_1}\boldsymbol{e}^{e_2 2\pi\, f_{20}x_2}\ldots\boldsymbol{e}^{e_n 2\pi\, f_{n0}x_n}, \tag{2}$$

i.e., the real signal low-pass signal $g(x)$ is multiplied by the n-D carrier $\mathrm{e}^{e_1 2\pi\, f_{10}x_1}\mathrm{e}^{e_2 2\pi\, f_{20}x_2}\ldots\mathrm{e}^{e_n 2\pi\, f_{n0}x_n}$ and all $f_{i0} \geq 0$, i=0, 1,..., n for the 1^{st} orthant quasi-analytic signals (denoted with subscript 1). Note that the appropriate change of signs of carrier frequencies f_{i0} yields quasi-analytic signals with spectra in other orthants of the frequency space. The signal (2) is called *complex* if $e_1 = e_2 = \ldots = e_n = j$ and $j^2 = -1$. The *hypercomplex quasi-analytic* signal is defined by a suitable choice of the algebra of basis vectors $e_1, e_2, \ldots, e_n$ [1]. The spectrum of (2) is shifted into the 1^{st} orthant of the n-D frequency space and has a general form

$$G_1(\boldsymbol{f}) = G(f_1 - f_{10}, f_2 - f_{20}, \ldots, f_n - f_{n0}). \tag{3}$$

Let us note that all carrier frequencies f_{i0}, $i = 1, 2, \ldots, n$ should be positive and big enough to shift the spectrum into the 1^{st} orthant with a negligible leakage into adjacent or-

*e-mail: snopek@ ire.pw.edu.pl

thants. As a measure of such a leakage, we propose the coefficient ε defined as

$$\varepsilon = 1 - \frac{\int\limits_{R^+} |G_1|^2 \, df}{\int\limits_{R^n} |G|^2 \, df} \tag{4}$$
$$= 1 - \frac{\text{Energy of (2) in the } 1^{st} \text{ orthant}}{\text{Total energy of } g(\boldsymbol{x})}.$$

It is observed that for quasi-analytic signals, ε is near 0. In the case when the support of the spectrum $G(\boldsymbol{f})$ is finite, it is possible to get $\varepsilon = 0$.

2. 2-D complex quasi-analytic signals

For n = 2, the formula (2) yields the $2-D$ *complex quasi-analytic signal*:

$$\psi_1(x_1, x_2) = g(x_1, x_2)\; e^{e_1 2\pi\, f_{10} x_1} e^{e_1 2\pi\, f_{20} x_2} \tag{5}$$

that is equivalent to

$$\begin{aligned}\psi_1(x_1, x_2) &= g(x_1, x_2)\left[c_1 c_2 - s_1 s_2 + e_1(s_1 c_2 + s_2 c_1)\right] \\ &= \mathrm{Re} + e_1 \mathrm{Im}\end{aligned} \tag{6}$$

Let us mention that in (6) and in the whole paper, we apply the following shortened notation: $c_i = \cos(\alpha_i)$, $s_i = \sin(\alpha_i)$, $\alpha_i = \alpha_i(x_i) = 2\pi f_{i0} x_i$, $i = 1, 2$. It can be shown that Hilbert transforms (total and partial [6–8]) of $u(x_1, x_2) = g(x_1, x_2) c_1 c_2$ in (6) are $v(x_1, x_2) \cong g(x_1, x_2) s_1 s_2$, $v_1(x_1, x_2) \cong g(x_1, x_2) s_1 c_2$ and $v_2(x_1, x_2) \cong g(x_1, x_2) c_1 s_2$, where the symbol "$\cong$" means "equals approximately". From (5), we get the spectrum of the 2-D quasi analytic signal:

$$G_1(\boldsymbol{f}) = G(f_1 - f_{10}, f_2 - f_{20}). \tag{7}$$

Let us illustrate the definition of the 2-D quasi-analytic signal and its spectrum with two examples of low-pass real signals: a 2-D Gaussian function and a rotated cuboid.

Example 1. The 2-D Gaussian function (in a normalized form) is given by

$$\begin{aligned}g(x_1, x_2) = &\frac{1}{2\pi\sigma_1\sigma_2\sqrt{1-\rho^2}} \\ &\cdot \exp\left[-\frac{\left(\frac{x_1}{\sigma_1}\right)^2 + \left(\frac{x_2}{\sigma_2}\right)^2 + 2\rho\frac{x_1 x_2}{\sigma_1\sigma_2}}{2(1-\rho^2)}\right],\end{aligned} \tag{8}$$

where σ_1, σ_2 are responsible for the spread in x_1 – and x_2 – domains and ρ is a correlation coefficient. Generally, (8) is a non-separable function of variables (x_1, x_2) but if $\rho = 0$, we get a separable one (a product of 1-D signals: $g(x_1, x_2) = g_1(x_1)\, g_2(x_2)$).

It is known that any 2-D signal can be represented as a union of four terms with different even-odd parity with respect to (w.r.t.) x_1 and x_2: $g = g_{ee} + g_{eo} + g_{oe} + g_{oo}$ ("e" denotes the even parity, "o" – the odd parity). However, low-pass signals are unions of only two terms: $g(x_1, x_2) = g_{ee}(x_1, x_2) + g_{oo}(x_1, x_2)$. Moreover, if $\rho = 0$, the odd-odd term vanishes. The Fourier spectrum of (8) is:

$$\begin{aligned}G(f_1, f_2) &= \exp\left[-0.5\left(\omega_1^2\sigma_1^2 + \omega_2^2\sigma_2^2 + 2\rho\omega_1\omega_2\sigma_1\sigma_2\right)\right] \\ &= G_{ee}(f_1, f_2) + G_{oo}(f_1, f_2),\end{aligned} \tag{9}$$

where

$$\begin{aligned}G_{ee}(f_1, f_2) = \exp&\left[-0.5\left(\omega_1^2\sigma_1^2 + \omega_2^2\sigma_2^2\right)\right] \\ &\cosh(\omega_1\omega_2\sigma_1\sigma_2\rho),\end{aligned} \tag{10}$$

$$\begin{aligned}G_{oo}(f_1, f_2) = \exp&\left[-0.5\left(\omega_1^2\sigma_1^2 + \omega_2^2\sigma_2^2\right)\right] \\ &\sinh(\omega_1\omega_2\sigma_1\sigma_2\rho).\end{aligned} \tag{11}$$

Figure 1a shows an even-even low-pass spectrum of the Gaussian function with $\sigma_1 = \sigma_2 = 0.5$, $\rho = 0 : G(f_1, f_2) = G_{ee}$. Remark that lines $x_1 = 0$ and $x_2 = 0$ in all figures should be treated as auxiliary. By an appropriate choice of values of f_{10}, f_{20} in (2) (here $f_{10} = f_{20} = 1.25$), we shift the spectrum into the 1^{st} quadrant ($f_1 > 0$, $f_2 > 0$) that is illustrated in Fig. 1b. Since the value of the parameter ε is near zero, the leakage of the spectrum into adjacent quadrants is very small.

a)

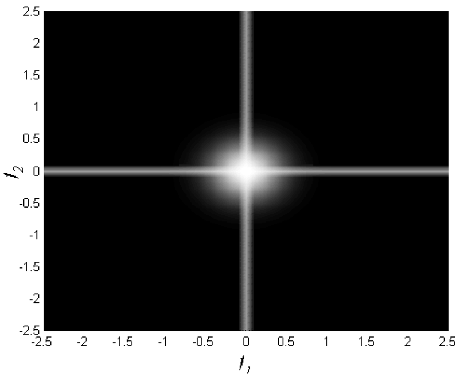

b)

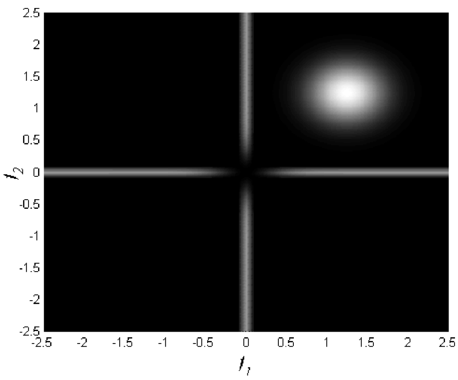

Fig. 1. (a) The spectrum $G(f_1, f_2)$ of the Gaussian function $\sigma_1 = \sigma_2 = 0.5$, $\rho = 0$; b) the shifted spectrum of (a): $G(f_1 - 1.25, f_2 - 1.25)$

Figure 2a shows the spectrum of the non-separable Gaussian function with $\sigma_1 = \sigma_2 = 0.7$, $\rho = 0.9$. It is a sum of even-even and odd-odd parts: $G(f_1, f_2) = G_{ee} + G_{oo}$ displayed respectively in Figs. 3a and b. In Fig. 2b we display the spectrum $G(f_1, f_2)$ shifted by $f_{10} = f_{20} = 1.25$ into the 1^{st} quadrant. The numerically calculated value of ε is 0.00054 and from the practical point of view the observed leakage of the spectrum is negligible.

Example 2. Let us present the next example of a rotated cuboid, with $a = b = 2$ (see Appendix A, Eq. (A1)). The support of this signal is displayed in Fig. 4a and its spectrum in Figs. 4b and c. The spectrum of the corresponding quasi-analytic signal given by (2), $f_{10} = f_{20} = 1.5$, is shown in Fig. 5. Due to the sharp edges of the cuboid, the oscillatory spectrum has a finite leakage into other quadrants with the numerically calculated value of the parameter $\varepsilon = 0.013$.

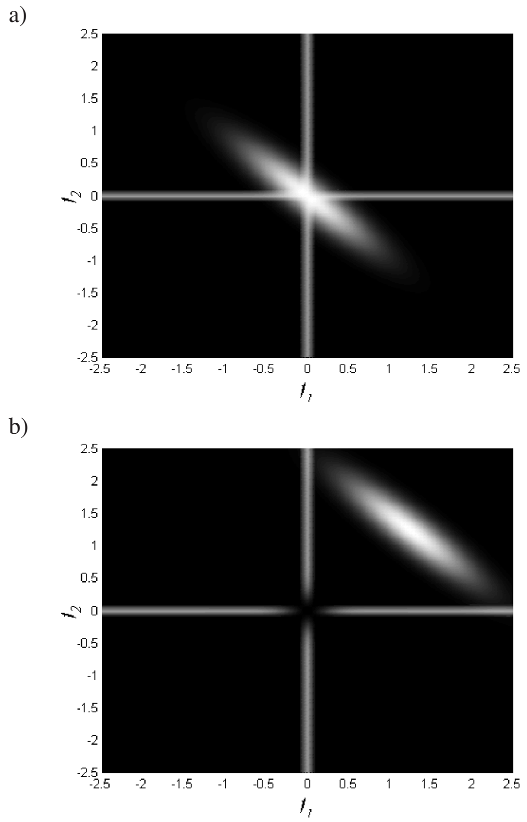

Fig. 2. (a) The spectrum of the Gaussian function σ_1= σ_2= 0.7, ρ = 0.9. (b) The shifted spectrum of (a): $G(f_1 - 1.25, f_2 - 1.25)$

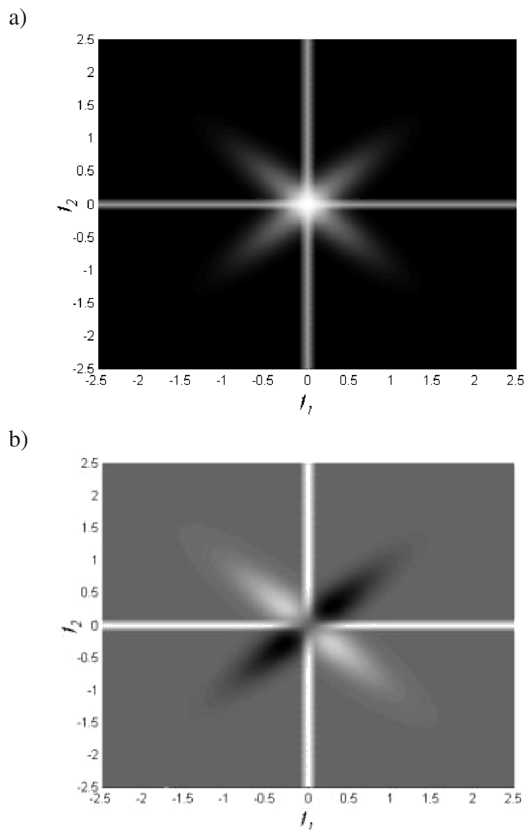

Fig. 3. The spectrum of Fig. 2a, a) the even-even part, b) the odd-odd part

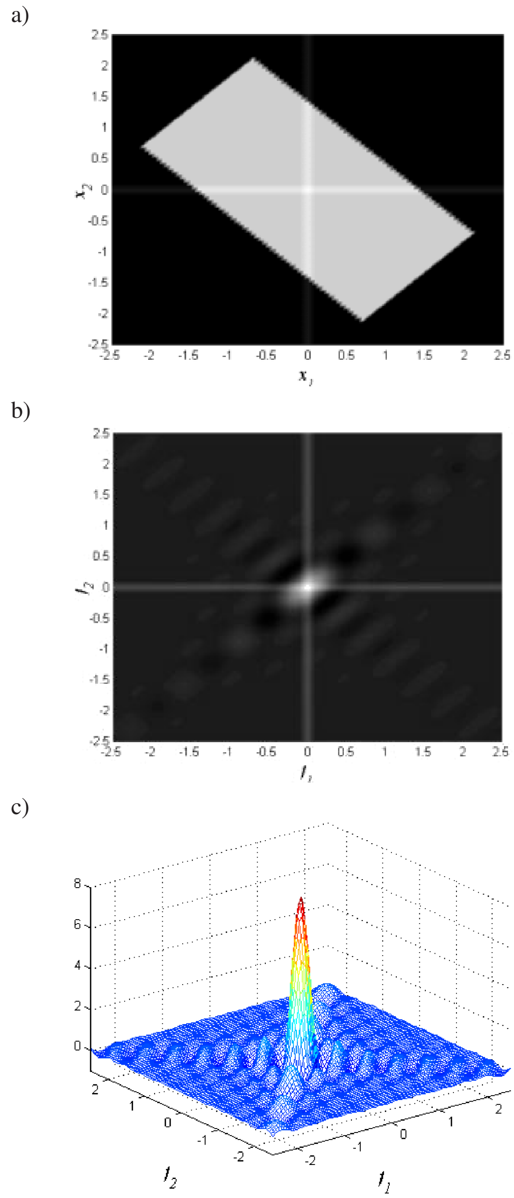

Fig. 4. A rotated cuboid: a) the support in $\boldsymbol{x}$-domain, b) the 2-D view of its spectrum, c) the 3-D view of the spectrum

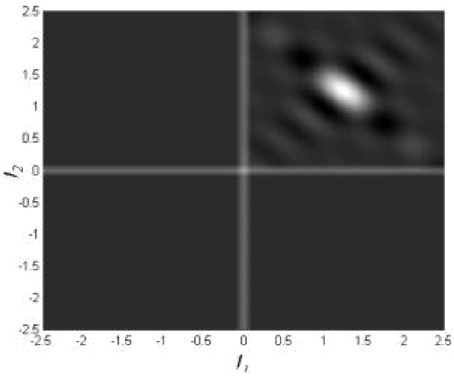

Fig. 5. The spectrum of the quasi-analytic signal of the rotated cuboid

2.1. Polar representation of 2-D complex quasi-analytic signals. Note that energies of low-pass signals in the non-separable case, Fig. 2a, are different in the 1^{st} ($f_1 > 0$, $f_2 > 0$) and in the 3^{rd} ($f_1 > 0$, $f_2 < 0$) quadrants. In consequence, the inverse Fourier transform of these two single-quadrant spectra defines two different analytic signals:

$$\begin{aligned}\psi_1(x_1, x_2) &= \mathcal{F}^{-1}\{1(f_1, f_2)\; G(f_1, f_2)\} \\ &= g - v + e_1(v_1 + v_2),\end{aligned} \tag{12}$$

$$\begin{aligned}\psi_3(x_1, x_2) &= \mathcal{F}^{-1}\{1(f_1, -f_2)\; G(f_1, f_2)\} \\ &= g + v + e_1(v_1 - v_2),\end{aligned} \tag{13}$$

where $g(x_1, x_2)$ is a 2-D real signal, $v(x_1, x_2)$ – its total Hilbert transform, $v_1(x_1, x_2)$, $v_2(x_1, x_2)$ – its partial Hilbert transforms w.r.t. x_1 and x_2 respectively [6–8]. The $1(f_1, f_2)$ is a 2-D unit step operator (as in (1)) yielding the single-quadrant support of the spectrum in the 1^{st} quadrant of R^2.

It is known that polar forms of complex analytic signals (12)–(13) uniquely define two different local amplitudes A_1, A_2 and two different phase functions Φ_1, Φ_2 [6–8], i.e.,

$$\psi_1(x_1, x_2) = A_1(x_1, x_2)\; e^{e_1\Phi_1(x_1,x_2)}, \tag{14}$$

$$\psi_3(x_1, x_2) = A_2(x_1, x_2)\; e^{e_1\Phi_2(x_1,x_2)}, \tag{15}$$

where

$$A_1(x_1, x_2) = \sqrt{\psi_1\psi_1^*} = \sqrt{(g-v)^2 + (v_1+v_2)^2}, \tag{16}$$

$$A_2(x_1, x_2) = \sqrt{\psi_3\psi_3^*} = \sqrt{(g+v)^2 + (v_1-v_2)^2}, \tag{17}$$

$$\Phi_1(x_1, x_2) = \tan^{-1}\left(\frac{v_1+v_2}{g-v}\right), \tag{18}$$

$$\Phi_2(x_1, x_2) = \tan^{-1}\left(\frac{v_1-v_2}{g+v}\right). \tag{19}$$

However, if $g(x_1, x_2)$ in (12)–(13) is a separable function, $g = g_1(x_1)\, g_2(x_2)$, its polar analytic form defines only one 2-D local amplitude: $A_1 = A_2 = A = \sqrt{g^2 + v^2 + v_1^2 + v_2^2}$ and two 2-D phase functions: $\Phi_1 = \alpha_1(x_1) + \alpha_2(x_2)$, $\Phi_2 = \alpha_1(x_1) - \alpha_2(x_2)$. In this case, the quasi-analytic signal (5) is also a separable function and can be represented by a single amplitude and two phase functions [6–8]:

$$\begin{aligned}\psi_1(x_1, x_2) &= A(x_1, x_2)\; e^{e_1\Phi(x_1,x_2)} \\ &= |g(x_1, x_2)|\; e^{e_1\Phi(x_1,x_2)},\end{aligned} \tag{20}$$

where

$$A(x_1, x_2) = \sqrt{\psi_1\psi_1^*} = \sqrt{Re^2 + Im^2} = |g(x_1, x_2)| \tag{21}$$

and

$$\tan(\Phi) = \tan\left(\frac{\mathrm{Im}}{\mathrm{Re}}\right) = \tan(\alpha_1 + \alpha_2). \tag{22}$$

From (22), we immediately get $\Phi = \alpha_1 + \alpha_2$. We observe that (20) differs from (5) since $g(x_1, x_2)$ has been replaced by its absolute value. However, in the case of unipolar positive baseband functions both functions are equal.

3. 2-D quaternion quasi-analytic signals

Differently to the real spectrum of the real signal $g(x_1, x_2)$, as e.g. that given by (8), the corresponding quaternion spectrum is a complex function:

$$G_q(f_1, f_2) = G_{ee}(f_1, f_2) + e_3 G_{oo}(f_1, f_2). \tag{23}$$

Note that if we want to define the quaternion quasi-analytic signal using (1) in a situation where both terms G_{ee} and G_{oo} exist, the even-even and odd-odd terms should be shifted into the 1^{st} quadrant separately.

The 2-D *quaternion quasi-analytic signal* (2) has the form

$$\psi_1^q(x_1, x_2) = g(x_1, x_2)\; e^{e_1\alpha_1} e^{e_2\alpha_2}, \tag{24}$$

i.e., in comparison to (5), in the second exponent, e_1 has been replaced by e_2. The superscript q means "quaternion". The developed form of (24) is

$$\begin{aligned}\psi_1^q(x_1, x_2) &= g(x_1, x_2) \\ &\cdot (c_1c_2 + e_1 s_1 c_2 + e_2 c_1 s_2 + e_3 s_1 s_2).\end{aligned} \tag{25}$$

3.1. Polar representation of 2-D quaternion quasi-analytic signals. Let us recall that the general polar representation of the quaternion analytic signal derived in [5] is

$$\begin{aligned}\psi_1^q(x_1, x_2) &= A(x_1, x_2) \\ &\cdot e^{e_1\Phi_1(x_1,x_2)} e^{e_3\Phi_3(x_1,x_2)} e^{e_2\Phi_2(x_1,x_2)}.\end{aligned} \tag{26}$$

where the 2-D amplitude

$$A(x_1, x_2) = \sqrt{\psi_1^q(\psi_1^q)^*} = |g(x_1, x_2)| \tag{27}$$

is the same as in (21) and three phase functions $\Phi_i(x_1, x_2)$ are defined by Euler angles and expressed as

$$\begin{aligned}\tan(2\Phi_1) &= \frac{2(uv_1 + vv_2)}{u^2 - v_1^2 + v_2^2 - v^2} \\ &= 2\frac{c_1c_2s_1c_2 + s_1s_2c_1s_2}{c_1^2c_2^2 - s_1^2c_2^2 + c_1^2s_2^2 - s_1^2s_2^2} \\ &= \frac{2\tan(\alpha_1)}{1 - \tan^2(\alpha_1)} = \tan(2\alpha_1),\end{aligned} \tag{28}$$

$$\begin{aligned}\tan(2\Phi_2) &= \frac{2(uv_2 + vv_1)}{u^2 - v_1^2 + v_2^2 - v^2} \\ &= 2\frac{c_1c_2c_1s_2 + s_1s_2s_1s_2}{c_1^2c_2^2 + s_1^2c_2^2 - c_1^2s_2^2 - s_1^2s_2^2} \\ &= \frac{2\tan(\alpha_2)}{1 - \tan^2(\alpha_2)} = \tan(2\alpha_2)\end{aligned} \tag{29}$$

$$\sin(\Phi_3) = \frac{uv - v_1 v_2}{A^2} = \frac{c_1 c_2 s_1 s_2 - s_1 s_2 c_1 s_2}{A^2} = 0. \tag{30}$$

As a result, we obtain $\Phi_1 = \alpha_1$, $\Phi_2 = \alpha_2$, $\Phi_3 = 0$ and finally

$$\psi_1^q(x_1, x_2) \approx |g(x_1, x_2)| \; e^{e_1 2\pi f_{10} x_1} e^{e_2 2\pi f_{20} x_2}, \tag{31}$$

that is, similarly to the complex case, we have only two phase functions expressed by Euler angles. We can easily show that the same result could be derived directly by comparison of (24) and (31).

4. Lower rank 2-D signals

The notion of the lower rank 2-D signal has been introduced in [1] in the form of a union of two signals (of rank 2) with single-quadrant spectra in the adjacent quadrants. For example, the 2-D signal of rank 1 has the spectrum limited to the half plane (HP) $f_1 > 0$ and is defined as the average of two signals with spectra in the 1^{st} and 3^{rd} quadrants respectively:

$$\psi_{HP}(x_1, x_2) = \frac{\psi_1 + \psi_3}{2} = \frac{\psi_1^q + \psi_3^q}{2} \\ = u(x_1, x_2) + e_1 v_1(x_1, x_2) = A_{HP} e^{e_1 \Phi_{HP}}. \tag{32}$$

where ψ_1 and ψ_3 are given by (14) and (15) and $\psi_1^q = u + e_1 v_1 + e_2 v_2 + e_3 v$ and $\psi_3^q = u + e_1 v_1 - e_2 v_2 - e_3 v$ [1]. So, the 2-D signals of rank 1 have the same form for complex and hypercomplex (quaternion) signals. Their amplitude is $A_{HP} = \sqrt{Re^2 + Im^2} = |g(x_1, x_2)| \, |\cos(\alpha_2)|$ and the phase is $\Phi_{HP}(x_1, x_2) = \alpha_1$.

5. 3-D complex quasi-analytic signals

Similarly to the 2-D case, a 3-D quasi-analytic signal is defined by the inverse Fourier transform (1) of a low-pass spectrum of a real signal shifted into a single octant. The complex quasi-analytic signal with single octant spectrum in the 1^{st} octant has the form

$$\psi_1(x_1, x_2, x_3) = g(x_1, x_2, x_3) \; e^{e_1 \alpha_1} e^{e_1 \alpha_2} e^{e_1 \alpha_3}, \tag{33}$$

where $\alpha_i = 2\pi f_{i0} x_i$, $i = 1, 2, 3$ and f_{i0} are three shift frequencies of the carrier. The developed form of (33) is

$$\psi_1(x_1, x_2, x_3) \\ = g(x_1, x_2, x_3)\left[c_1 c_2 c_3 - s_1 s_2 c_3 - s_1 c_2 s_3 - c_1 s_2 s_3 \right. \\ \left. + e_1(s_1 c_2 c_3 + c_1 s_2 c_3 + c_1 c_2 s_3 - s_1 s_2 s_3)\right]. \tag{34}$$

Consider the example with a 3-D non-separable Gaussian function defined by three variances σ_1, σ_2, σ_3 and three correlation coefficients ρ_{12}, ρ_{13}, ρ_{23}. A specific example of the Gauss function spectrum presented in Figs. 7a and b shows the cross-section of the spectrum of Fig. 5a shifted into the 1^{st} octant (Remark: we present only a chosen cross-section of a 3-D spectrum).

Let us recall that a 3-D signal $g(x_1, x_2, x_3)$ may be represented as a sum of eight terms with different parity (even/odd). However, for low-pass real signals g, we have a sum of four terms only [1]:

$$g(x_1, x_2, x_3) = g_{eee} + g_{eoo} + g_{oeo} + g_{ooe} \tag{35}$$

with the spectrum given by

$$G(f_1, f_2, f_3) = G_{eee} - G_{eoo} - G_{oeo} - G_{ooe}. \tag{36}$$

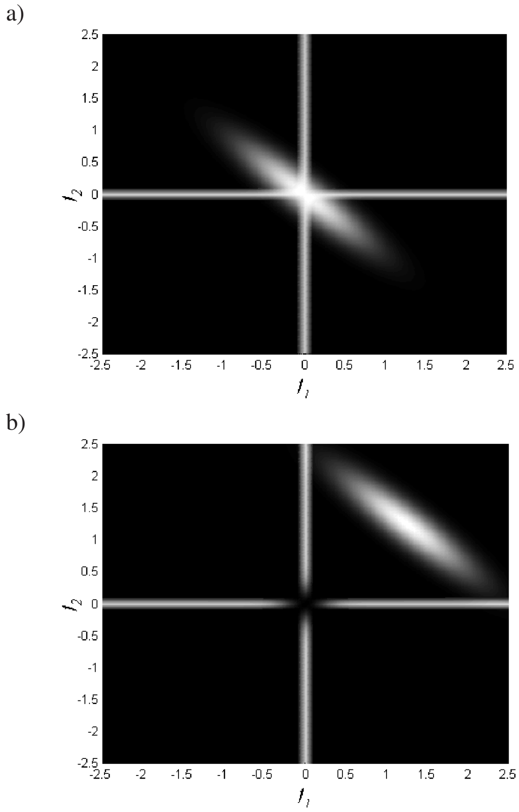

Fig. 6. a) The cross-section $G(f_1,\, f_2,\, f_3 = 0)$ of the spectrum of the low-pass 3-D Gaussian function $\sigma_1 = \sigma_2 = \sigma_3 = 0.7$, $\rho_{12} = \rho_{13} = \rho_{23} = 0.9$, b) the shifted spectrum of (a): $G(f_1 - 1.25,\, f_2 - 1.25,\, f_3 = 0)$, leakage $\varepsilon = 0.0000$

First, let us compare the 3-D analytic and quasi-analytic signals in the complex case. It is evident that the half-space $f_1 > 0$ is divided into four octants labeled 1, 3, 5 and 7 [6]. Their energies in successive octants may differ. In consequence, a real signal g is represented by four different analytic signals with single-octant spectra denoted ψ_1, ψ_3, ψ_5 and ψ_7 (of different energies). For example, the signal ψ_1 with the spectrum limited to the 1^{st} octant is

$$\psi_1(x_1, x_2, x_3) = g - v_{12} - v_{13} - v_{23} \\ + e_1(v_1 + v_2 + v_3 - v), \tag{37}$$

where notations are similar as in the 2-D case: v_i denotes the first-order partial Hilbert transforms of g w.r.t. a single variable x_i and v_{ij}, the second-order partial Hilbert transform w.r.t. two corresponding variables x_i and x_j The signals ψ_3, ψ_5 and ψ_7 differ only by signs of the sum [6–8]. In consequence, their definitions differ from (37) only by signs in exponents. They are defined by the same local amplitude.

Polar Representation of 3-D Complex Quasi-Analytic Signals. The polar forms of four complex analytic signal define four amplitudes and four phase functions. For separable signals, all four amplitudes are equal:

$$A(x_1,x_2,x_3)=\sqrt{\psi_1\psi_1^*}=\sqrt{\mathrm{Re}^2+\mathrm{Im}^2}=|g(x_1,x_2,x_3)| \tag{38}$$

and the four phase functions are [6]

$$\Phi_1=\alpha_1+\alpha_2+\alpha_3, \tag{39}$$

$$\Phi_3=\alpha_1-\alpha_2+\alpha_3, \tag{40}$$

$$\Phi_5=\alpha_1+\alpha_2-\alpha_3, \tag{41}$$

$$\Phi_7=\alpha_1-\alpha_2-\alpha_3 \tag{42}$$

where Φ_1 is defined by

$$\tan(\Phi_1)=\frac{s_1c_2c_3+c_1s_2c_3+c_1c_2s_3-s_1s_2s_3}{c_1c_2c_3-s_1s_2c_3-s_1c_2s_3-c_1s_2s_3}=\tan(\alpha_1+\alpha_2+\alpha_3). \tag{43}$$

Analogously,

$$\tan(\Phi_3)=\frac{s_1c_2c_3-c_1s_2c_3+c_1c_2s_3+s_1s_2s_3}{c_1c_2c_3+s_1s_2c_3-s_1c_2s_3+c_1s_2s_3}=\tan(\alpha_1-\alpha_2+\alpha_3), \tag{44}$$

$$\tan(\Phi_5)=\frac{s_1c_2c_3+c_1s_2c_3-c_1c_2s_3+s_1s_2s_3}{c_1c_2c_3-s_1s_2c_3+s_1c_2s_3+c_1s_2s_3}=\tan(\alpha_1+\alpha_2-\alpha_3) \tag{45}$$

and

$$\tan(\Phi_7)=\frac{s_1c_2c_3-c_1s_2c_3-c_1c_2s_3-s_1s_2s_3}{c_1c_2c_3+s_1s_2c_3+s_1c_2s_3-c_1s_2s_3}=\tan(\alpha_1+\alpha_2+\alpha_3). \tag{46}$$

6. 3-D hypercomplex quasi-analytic signals

6.1. Cayley-Dickson algebra. The 3-D quasi-analytic hypercomplex signal [1] defined by the Cayley-Dickson (CD) algebra of unit vectors (see Appendix B) is

$$\psi_1^{CD}(x_1,x_2,x_3)=g(x_1,x_2,x_3)\ e^{e_1\alpha_1}e^{e_2\alpha_2}e^{e_4\alpha_3}. \tag{47}$$

Note the special order of imaginary units in (47): e_1, e_2, e_4. The developed form of (47) is

$$\psi_1^{CD}(x_1,x_2,x_3)=g(x_1,x_2,x_3)\ (c_1c_2c_3+e_1s_1c_2c_3+e_2c_1s_2c_3+e_3s_1s_2c_3+e_4c_1c_2s_3+e_5s_1c_2s_3+e_6c_1s_2s_3\pm e_7s_1s_2s_3). \tag{48}$$

Remark. The sign of e_7 depends on the order of multiplication.

6.2. Clifford algebra. The 3-D quasi-analytic signal defined by the Clifford (Cl) algebra of unit vectors (see Appendix C) is

$$\psi_1^{Cl}(x_1,x_2,x_3)=g(x_1,x_2,x_3)\ e^{e_1\alpha_1}e^{e_2\alpha_2}e^{e_3\alpha_3}. \tag{49}$$

In comparison to (47), the order is e_1, e_2, e_3 and the developed form of (49) is

$$\psi_1^{Cl}(x_1,x_2,x_3)=g(x_1,x_2,x_3)\cdot[c_1c_2c_3+e_1s_1c_2c_3+e_2c_1s_2c_3+(e_1e_2)s_1s_2c_3+e_3c_1c_2s_3+(e_1e_3)s_1c_2s_3+(e_2e_3)c_1s_2s_3+\omega s_1s_2s_3], \tag{50}$$

where $\omega=e_1e_2e_3$ and in the Clifford algebra $\omega^2=+1$ (and not -1) (see Appendix C). Assuming that the amplitude should be a unipolar positive function, the polar form of (50) is undefined, since $\psi_1^{Cl}\left(\psi_1^{Cl}\right)^*=g^2(x_1,x_2,x_3)\left(1-2s_1^2s_2^2s_3^2\right)$ is a bipolar function.

6.3. Polar representation of 3-D hypercomplex quasi-analytic signals. The problem of the polar representation of 3-D hypercomplex analytic signals has been discussed in [1]. In principle, the 3-D hypercomplex signal with a single-octant spectrum is represented by a single amplitude and seven phase functions. However, if the signal is a separable function, we have only three phase functions. Since quasi-analytic signals are separable functions, the signal (47) is represented by three phase functions. Its amplitude is

$$A(x_1,x_2,x_3)=\sqrt{\psi_1^{CD}\left(\psi_1^{CD}\right)^*}=|g(x_1,x_2,x_3)| \tag{51}$$

and the three phase angles, as shown in [1], are α_1, α_2, α_3. Therefore, finally we have

$$\psi_1^{CD}(x_1,x_2,x_3)=|g(x_1,x_2,x_3)|\ e^{e_1\alpha_1}e^{e_2\alpha_2}e^{e_4\alpha_3}. \tag{52}$$

7. Lower rank 3-D signals

The above described 3-D signals have the rank equal 3. Let us derive the formulae defining signals of rank 2.

Complex case: The complex signal (33) has the spectral support in the 1^{st} octant. Let us write signals with spectral supports in the octants No. 3, 5 and 7: $\psi_3=ge^{e_1\alpha_1}e^{-e_1\alpha_2}e^{e_1\alpha_3}$, $\psi_5=ge^{e_1\alpha_1}e^{e_1\alpha_2}e^{-e_1\alpha_3}$ and $\psi_7=ge^{e_1\alpha_1}e^{-e_1\alpha_2}e^{-e_1\alpha_3}$. The signals of rank 2 are given by

$$\psi_{1+5}(x_1,x_2,x_3)=\frac{\psi_1+\psi_5}{2}=ge^{e_1\alpha_1}e^{e_1\alpha_2}\cos(\alpha_3)=A_{1+5}e^{e_1\Phi_{1+5}}, \tag{53}$$

$$\psi_{3+7}(x_1,x_2,x_3)=\frac{\psi_3+\psi_7}{2}=ge^{e_1\alpha_1}e^{-e_1\alpha_2}\cos(\alpha_3)=A_{3+7}e^{e_1\Phi_{3+7}}. \tag{54}$$

Their amplitudes are the same: $A_{1+5}=A_{3+7}=|g|\,|\cos(\alpha_3)|$ and the phase functions respectively are $\Phi_{1+5}=\alpha_1+\alpha_2$, $\Phi_{3+7}=\alpha_1-\alpha_2$. The rank-1 signal with the spectrum support in the half space (HS) $f_1>0$ is

$$\psi_{HS}(x_1,x_2,x_3)=\frac{\psi_{1+5}+\psi_{3+7}}{2}=g\cos(\alpha_2)\cos(\alpha_3)\ e^{e_1\alpha_1}=A_{HS}e^{e_1\Phi_{HS}}. \tag{55}$$

Its amplitude $A_{HS}=|g|\,|\cos(\alpha_2)|\,|\cos(\alpha_3)|$ and the phase function is $\Phi_{HS}=\alpha_1$.

Octonion case (Cayley-Dickson algebra). The hypercomplex signal (44) has the spectral support in the 1^{st} octant. Let us recall the general forms of signals with spectral supports in the octants No. 3, 5, 7: $\psi_3^{CD}=ge^{e_1\alpha_1}e^{-e_2\alpha_2}e^{e_4\alpha_3}$, $\psi_5^{CD}=$

$ge^{e_1\alpha_1}e^{e_2\alpha_2}e^{-e_4\alpha_3}$ and $\psi_7^{CD} = ge^{e_1\alpha_1}e^{-e_2\alpha_2}e^{-e_4\alpha_3}$. The signals of rank 2 are defined by

$$\psi_{1+5}^{CD}(x_1, x_2, x_3) = \frac{\psi_1^{CD} + \psi_5^{CD}}{2} = ge^{e_1\alpha_1}e^{e_2\alpha_2}\cos(\alpha_3) = A_{1+5}e^{e_1\phi_{1+5}^{(1)}}e^{e_2\phi_{1+5}^{(2)}}, \tag{56}$$

$$\psi_{3+7}^{CD}(x_1, x_2, x_3) = \frac{\psi_3^{CD} + \psi_7^{CD}}{2} = ge^{e_1\alpha_1}e^{-e_2\alpha_2}\cos(\alpha_3) = A_{3+7}e^{e_1\phi_{3+7}^{(1)}}e^{-e_2\phi_{3+7}^{(2)}}. \tag{57}$$

Their amplitudes are the same as in (53) and (54) and the phase functions expressed by Euler angles given by (28)–(30) are $\phi_{1+5}^{(1)}(x_1, x_2, x_3) = \phi_{3+7}^{(1)} = \alpha_1$, $\phi_{1+5}^{(2)}(x_1, x_2, x_3) = -\phi_{3+7}^{(2)} = \alpha_2$. Of course, the phase angles are defined directly by the comparison of exponents in (53) and (54). However, using the Euler angles (28)–(30) we can show that the same formulae apply for quaternions with 3-D terms. The rank-1 signals are again the same for complex and octonion signals. We have

$$\psi_{HS}(x_1, x_2, x_3) = \frac{\psi_{1+5}^{CD} + \psi_{3+7}^{CD}}{2} = g\cos(\alpha_2)\cos(\alpha_3)\ e^{e_1\alpha_1} = A_{HS}e^{e_1\Phi_{HS}}. \tag{58}$$

The amplitude is $A_{HS} = |g|\,|\cos(\alpha_2)|\,|\cos(\alpha_3)|$ and the phase $\Phi_{HS} = \alpha_1$.

8. Conclusions

Quasi-analytic signals with single-orthant spectra have been defined by multiplication of a low-pass (baseband) – n-D signal $g(x_1, x_2, \ldots, x_n)$ by a multidimensional carrier (complex or hypercomplex). This operation should shift the low-pass spectrum of g into a single-orthant. The leakage of the energy of the modulated signal into other orthants of the frequency space should be negligible. The measure of this leakage has been introduced.

From the point of view of the polar representation, the 2-D and 3-D quasi-analytic signals of non-separable low-pass signals have the analogous polar representation as separable functions: We have a single amplitude and two (in 2-D) or three (in 3-D) phase functions.

Appendix A. The spectrum of the rotated cuboid

The spectrum of the cuboid is well known. For convenience, let us recall the definition of a cuboid. The symmetric cuboid (non-rotated) is defined as a product of two rectangles

$$g(x_1, x_2) = \Pi_a(x_1)\,\Pi_b(x_2), \tag{A1}$$

where

$$\Pi_a(x_1) = \begin{cases} 1, & |x_1| < a \\ 0.5, & |x_1| = \pm a \\ 0, & |x_1| > a \end{cases},$$

$$\Pi_b(x_2) = \begin{cases} 1, & |x_2| < b \\ 0.5, & |x_2| = \pm b \\ 0, & |x_2| > b \end{cases}.$$

The Fourier spectrum of (A1) is

$$G(f_1, f_2) = 2a\frac{\sin(2\pi f_1 a)}{2\pi f_1 a}2b\frac{\sin(2\pi f_2 b)}{2\pi f_2 b}. \tag{A2}$$

Of course, $g$and G are separable 2-D functions. The rotated cuboid defined in a coordinate system rotated by the angle γ is non-separable. As well, the spectrum of the rotated cuboid defined by rotation of the frequency domain coordinate system is also a non-separable function.

Appendix B. The Cayley-Dickson algebra

The Cayley-Dickson multiplication rules of unit vectors are presented in Table 1. Details concerning the Cayley-Dickson algebra are presented in [1] or in many other sources. Note that the part of the table for e_1, e_2 and e_3 presents multiplication rules of quaternions.

Table 1
Multiplication rules in the algebra of octonions

$\times$	*1*	e_1	e_2	e_3	e_4	e_5	e_6	e_7
1	1	e_1	e_2	e_3	e_4	e_5	e_6	e_7
e_1	e_1	-1	e_3	$-e_2$	e_5	$-e_4$	$-e_7$	e_6
e_2	e_2	$-e_3$	-1	e_1	e_6	e_7	$-e_4$	$-e_5$
e_3	e_3	e_2	$-e_1$	-1	e_7	$-e_6$	e_5	$-e_4$
e_4	e_4	$-e_5$	$-e_6$	$-e_7$	-1	e_1	e_2	e_3
e_5	e_5	e_4	$-e_7$	e_6	$-e_1$	-1	$-e_3$	e_2
e_6	e_6	e_7	e_4	$-e_5$	$-e_2$	e_3	-1	$-e_1$
e_7	e_7	$-e_6$	e_5	e_4	$-e_3$	$-e_2$	e_1	-1

Appendix C. The Clifford algebra $Cl_{0,3}(P)$

The rules of multiplication of unit vectors of the Clifford algebra $Cl_{0,3}(P)$ are given in Table 2. Details can be found in [1] or in other sources.

Table 2
Multiplication rules In $Cl_{0,3}(P)$

$\times$	**1**	e_1	e_2	e_3	e_1e_2	e_1e_3	e_2e_3	ω
1	1	e_1	e_2	e_3	e_1e_2	e_1e_3	e_2e_3	ω
e_1	e_1	-1	e_1e_2	e_1e_3	$-e_2$	$-e_3$	ω	$-e_2e_3$
e_2	e_2	$-e_1e_2$	-1	e_2e_3	e_1	$-\omega$	$-e_3$	e_1e_3
e_3	e_3	$-e_1e_3$	$-e_2e_3$	-1	$-\omega$	e_1	e_2	e_1e_2
e_1e_2	e_1e_2	e_2	$-e_1$	ω	-1	e_2e_3	$-e_1e_3$	$-e_3$
e_1e_3	e_1e_3	e_3	ω	$-e_1$	$-e_2e_3$	-1	e_1e_2	$-e_2$
e_2e_3	e_2e_3	$-\omega$	e_3	$-e_2$	e_1e_3	$-e_1e_2$	-1	e_1
ω	ω	e_2e_3	$-e_1e_3$	$-e_1e_2$	e_3	e_2	$-e_1$	1

REFERENCES

[1] K.M. Snopek and S.L. Hahn, "The unified theory of n-dimensional complex and hypercomplex analytic signals", *Bull. Polish Ac.: Tech.* 59 (2), 167–181 (2011).

[2] S.J. Sangwine and N. Le Bihan, *Hypercomplex Analytic Signals: Extension of the Analytic Signal Concept to Complex Signals,* EUSIPCO, Poznań, 2007.

[3] C. Wachinger, T. Klein, and N. Navab, "The 2D analytic signal for envelope detection and feature extraction on ultrasound images", *Medical Image Analysis* 16, 1073–1084 (2012).

[4] T. Bülow and G. Sommer, *A Novel Approach to the 2D Analytic Signal*, pp. 25–32, Springer Verlag Berlin, 1999.

[5] T. Bülow and G. Sommer, "The hypercomplex signal – a novel extension of the analytic signal to the multidimensional case", *IEEE Trans. Signal Processing* 49 (11), 2844–2852 (2001).

[6] S.L. Hahn, "Multidimensional complex signals with single-orthant spectra", *Proc. IEEE* 80 (8), 1287–1300 (1992).

[7] S.L. Hahn, *Hilbert Transforms in Signal Processing*, Artech House Inc., London, 1996.

[8] S. Hahn, "Hilbert Transforms" in *The Transforms and Applications Handbook*, CRC Press, Orlando, 2010.

[9] C. Höhne, R. Boehm, and J. Prager, "Application of 2-dimensional analytic signals with single-orthant spectra for processing of SAFT-reconstructed images", in *Multidim. Syst. Sign. Process.*, Springer Science+Business Media, New York, 2013.

[10] S.J. Sangwine, C.J. Evans, and T.A. Ell, "Colour-sensitive edge detection using hypercomplex filters", *Proc. 10th Eur. Signal Processing Conf. EUSIPCO* 1, 107–110 (2000).

[11] D S. Alexiadis and G.D. Sergiadis, "Estimation of motions in color image sequences using hypercomplex Fourier transforms", *IEEE Trans. Image Processing* 18 (1), 168-187 (2009).

[12] T. Bulow, M. Felsberg, and G. Sommer, "Non-commutative hypercomplex Fourier transforms of multidimensional signals" in *Geometric Computing with Clifford Algebras*, ed. G. Sommer, pp. 187–207, Springer, Berlin, 2001.

[13] T.A. Ell and S.J. Sangwine, "Hypercomplex Fourier transforms of color images", *IEEE Trans. Image Process*, 16 (1), 22–35, (2007).

[14] S.L. Hahn and K.M. Snopek, "Comparison of properties of analytic, quaternionic and monogenic 2-D signals*", WSEAS Transactions on Computers* 3 (3), 602–611 (2004).